Somatosensory rhythms and cerebellar-basal ganglia beta-band interactions in Parkinson's disease

Victor Pando-Naude, MD, PhD [1] & Lau Møller Andersen, PhD [2,3]*

[1] Department of Clinical Medicine, Center for Music in the Brain, Aarhus University and The Royal Academy of Music Aarhus/Aalborg, Universitetsbyen, 3-0-17, 8000, Aarhus C, Denmark

[2] Center of Functionally Integrative Neuroscience (CFIN), Aarhus University, Universitetsbyen 3, Building 1710, 8000 Aarhus C, Denmark

[3] Department for Linguistics, Cognitive Science and Semiotics, Aarhus University, Jens Chr. Skous Vej 2, Building 1485, 8000 Aarhus C, Denmark

*Corresponding author

Lau Møller Andersen

Address: Universitetsbyen, 3-0-17, 8000, Aarhus C, Denmark

Telephone: +45 87169032

Email: lmandersen@cc.au.dk

ORCID: LMA - https://orcid.org/0000-0001-7323-0614; VPN - https://orcid.org/0000-0003-1963-5068

Word count: 4,944

Running title: Cerebellar timing in Parkinson's disease

Funding agencies: V.P.N. is funded by the Center for Music in the Brain (MIB), supported by the Danish National Research Foundation (DNRF 117). L.M.A. was funded by the Lundbeck Foundation (R322-2019-1841). The funders had no role in study design, data collection and analysis, decision to publish, or preparation of the manuscript.

Conflict of Interest: The authors declare no conflict of interest for this work.

Classification: Biological science - Neuroscience

Keywords: Cerebellum, Basal Ganglia, Somatosensory, Timing, Parkinson's Disease, Beta-Band

Abstract

Rhythmic cognition relies on the interplay between endogenous and exogenous temporal structures, allowing organisms to anticipate and adapt to events in time. Neural oscillations, particularly in the beta band (14-30 Hz), are central to this predictive capacity, coordinating sensorimotor networks that support timing and rhythm perception. Parkinson's disease, a movement disorder characterized by disrupted basal ganglia function, offers a unique framework to probe the neural mechanisms underlying rhythmic cognition. We measured beta-band activity and connectivity across cerebellum, basal ganglia, thalamus and motor cortex during a rhythmic somatosensory timing task to compare prediction- and evaluation-related activity between participants with Parkinson's disease and controls. Using magnetoencephalography, participants received tactile stimuli in regular (non-jittered) and irregular (jittered) sequences, with the final stimulus omitted to probe prediction *before* and evaluation *after* the omission. We found prediction-related differences between participants with Parkinson's disease and controls in cerebellum and basal ganglia *before* the omissions, while replicating earlier findings in controls, showcasing cerebellar evaluation responses *after* the omissions. In Parkinson's disease, basal ganglia activity favored jittered over non-jittered somatosensory rhythms, opposite to controls. Altered cerebellar beta-band responses correlated with Parkinson's disease symptom severity. Connectivity analyses revealed group-by-regularity interactions in a sensory-integration network. These findings demonstrate that temporal prediction and evaluation in rhythmic cognition rely on coordinated beta-band dynamics across the cerebello-striatal-thalamo-cortical network. In Parkinson's disease, disrupted basal ganglia function shifts the network toward compensatory cerebellar engagement and increased connectivity demands under irregular temporal conditions, exposing core mechanisms by which the brain encodes and adapts to rhythmic structure.

1. Introduction

Rhythms—whether externally perceived or internally generated—allow organisms to predict future states of the environment. Across modalities – visual, auditory, and somatosensory – predictive mechanisms support fundamental cognitive functions such as perception, attention, and action by enabling the brain to anticipate and adapt to upcoming events in time [1,2].. Rhythmic cognition refers to this capacity to couple endogenous neural oscillations with exogenous rhythms, forming predictive models that optimize sensorimotor behavior. Central to this process are prediction–evaluation cycles, whereby temporal expectations are generated, monitored, and updated when incoming sensory information confirms or violates those expectations. Neural oscillations, particularly in the beta band (14–30 Hz), have been identified as a key mechanism supporting these predictive dynamics across sensory and motor domains [3].

Two subcortical structures—the cerebellum and the basal ganglia—are central to rhythmic cognition. The cerebellum has long been implicated in generating internal forward models of sensory feedback [4,5], particularly in the somatosensory domain [6], allowing precise temporal prediction and evaluation of incoming signal [7,8]; while the basal ganglia are critical for interval timing, beat-based processing, and entrainment to regular rhythms, interacting with cortical motor areas to refine temporal predictions and support rhythmic behaviors [9–11].

Studies using magnetoencephalography (MEG) show that the cerebellum responds not only to tactile stimuli but also to the omission of expected stimuli, supporting its involvement in maintaining temporal predictions [12,13]. While debates persist about the differential roles of the basal ganglia and the cerebellum in timing operations, a theory proposes that the basal ganglia are responsible for supra-second timing while the cerebellum manages sub-second timing [14]. Alternatively, the basal ganglia may handle regular time intervals while the cerebellum processes irregular time intervals [15,16]. In Andersen & Dalal (2024b) [17], we offered yet another view, arguing that the basal ganglia perform core timing computations, while the cerebellum integrates timing information with spatial and sensory cues to generate spatiotemporal predictions. Our model emphasizes that the cerebellum is not directly involved in timing per se but serves as an integrative hub within a broader basal ganglia-cerebellum-thalamus-M1 system [17]. This integrated network plays a fundamental role in *predicting* when, where, and what sensory stimuli will occur. From this it follows that timing capabilities may thus be lost due to incapacitation of *either* basal ganglia *or* cerebellum, as also indicated by a recent lesion study [18]. Thus, one might conjecture that neurodegenerative diseases associated with loss of motor control and rhythmicity, such as Parkinson's disease (PD), would be associated with dysfunction in prediction mechanisms [19,20] due to altered cerebellar-basal ganglia interactions.

We previously showed that cerebellar beta-band responses to omitted tactile stimuli are modulated by the regularity of preceding input, with stronger responses following non-jittered rhythms, reflecting prediction evaluation [12]. This activity correlates with detection accuracy [21], suggesting that cerebellar dysfunction may impair predictive mechanisms critical for smooth movement in PD [22–25]. PD is primarily characterized by dopaminergic degeneration in the substantia nigra pars compacta, disrupting basal ganglia-thalamo-cortical circuitry and impairing motor functions [26,27], including timing [28]. By comparing participants with PD to controls, we can gain insights into the fundamental mechanisms of (1) sensory processing, (2) temporal prediction and evaluation, and (3) cerebellar beta-band activity [29]. At the same time, this comparison can help reveal potential cerebellar dysfunction specifically linked to PD. To meet these ends, we used MEG.

Due to its unmatched temporal resolution, MEG allows precise differentiation of activity occurring *before* versus *after* an expected but omitted stimulus. MEG captures millisecond-scale neural dynamics, complementing the high spatial but limited temporal resolution of magnetic resonance imaging. MEG has traditionally been regarded as mainly sensitive to the cerebral cortex, but recently it has been shown that the cerebellum is within reach of MEG [30,31]. The sensitivity of MEG to the basal ganglia, on the other hand,

is low, especially in situations where the cerebral cortex is activated simultaneously [32]. However, accumulating evidence suggests that subcortical contributions are detectable under appropriate conditions. Computational modeling studies demonstrate that the basal ganglia can generate measurable magnetic fields [32,33], and empirical findings indicate basal ganglia involvement in timing tasks captured with MEG [23,34]. Importantly, omission paradigms reduce concurrent cortical activity, thereby increasing sensitivity to subcortical signals. These advances support the validity of using MEG to examine basal ganglia dynamics in the current paradigm.[33,35].

This study aims to investigate cerebellar dysfunction in PD, focusing on the role of cerebellar beta-band activity in somatosensory prediction. Using MEG, we examine beta-band activity in response to regular (non-jittered) and irregular (jittered) sequences of tactile stimuli and omissions, comparing participants with PD to controls without PD. Due to the temporal resolution of MEG, we can tell apart effects that happen *before* the expected but omitted stimulus, i.e. related to the *prediction* of upcoming stimuli, from effects that happen *after* the expected but omitted stimulus, i.e. related to the *evaluation* of predictions.

The hypotheses of interest were:

1. Participants with PD exhibit altered cerebellar beta-band responses to omitted tactile stimuli in jittered versus non-jittered rhythms, i.e. an interaction between group and regularity of stimulation.
2. Participants with PD show altered basal ganglia beta-band activity during predictable somatosensory stimulation, indicating disrupted timing mechanisms.

For exploratory reasons we also estimated the functional connectivity in the beta-band between the cerebellum, the basal ganglia, the thalamus and the primary motor cortex. We have suggested that these areas together comprise a temporal integration network enabling proactive action [17]. The basal ganglia provide the temporal information; the cerebellum integrates the temporal information with other kinds of information, such as spatial information and intensity information, into predictions; and the thalamus [21] passes that information on to primary motor cortex to enable proactive action.

In this study, we found differential basal ganglia activations to omissions between participants with PD and controls. We believe that the veracity of this differential activation is supported by: **(1)** a beat-based somatosensory rhythmic timing paradigm, which preferentially activates the basal ganglia [15,16]; **(2)** omissions to elicit activity, which do not activate the cerebral cortex to the same degree that sensory stimulation does, thus, the MEG signal of the basal ganglia is more likely to be visible [32]; and **(3)** basal ganglia activation being expected to be altered in PD.

2. Results

MEG was recorded while 24 participants with PD and 25 age-matched controls, all right-handed, passively received right-index finger electrical pulse trains (**Figure 1**, **Table 1**). Each train comprised six 100-µs electrical stimuli separated by 1.497 s; in the non-jittered (0 %) condition all pulses were on time, whereas in the jittered (15 %) condition, pulses 4–6 were shifted randomly by ±225 ms, and the seventh event was always omitted to probe predictive processing. Participants fixated on a silent nature film to minimize eye and body movements. MEG signals were band-passed at 14–30 Hz (beta band), epoched around each stimulus or omission, and reconstructed to source space with linearly constrained minimum-variance beamforming. Condition- and group-dependent beta-power and envelope-correlation metrics were then extracted for cerebellum, basal ganglia, thalamus and primary motor cortex, as proposed by Andersen & Dalal (2024b) [17].

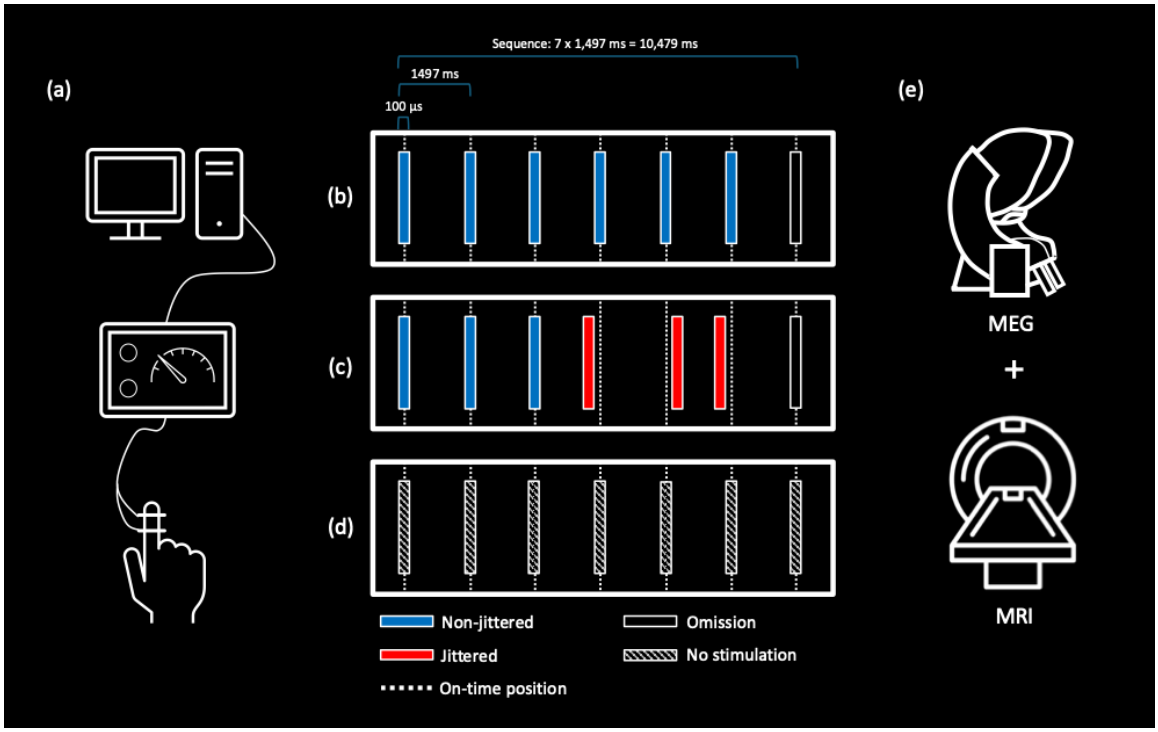

Figure 1. Experimental paradigm. (a) *Tactile stimuli were administered via ring electrodes placed on the right index finger, delivering sequences of six pulses with a duration of 100 µs and inter-stimulus interval of 1,497ms. PsychoPy controlled the stimulation, while participants watched a nature program and remained motionless. EOG, ECG, and EMG recordings were collected to monitor eye movements, heart activity, and neck muscle tension. Stimulus sequences included* ***(b)*** *non-jittered somatosensory rhythms,* ***(c)*** *jittered somatosensory rhythms (15%), and* ***(d)*** *non-stimulation sequences.* ***(e)*** *MEG was acquired during the paradigm and structural MRI was acquired another day within the next two weeks.*

Table 1. Demographics

	Controls	PD
Participants (n)	25	24
Gender (females)	16	8
Age (mean/SD years)	60.2 ± 9.43	66.0 ± 7.77
MDI (median/range points)	3 (0-19)	8 (0-17)
MoCA (median/range points)	29 (26-30)	29 (26-30)
PD dx (median/range years)	-	4 (1-17)
UPDRS-III (median/range points)	-	31 (13-47)
Hoehn and Yahr (median/range points)	-	2 (1-2)

PD, Parkinson's disease; MDI, Major Depression Inventory; MoCA, Montreal Cognitive Assessment; PD dx, years since PD diagnosis; UPDRS-III, Motor Examination of the Movement Disorder Society Unified Parkinson's Disease Rating Scale.

As an initial validation of our data processing pipeline, we analyzed evoked responses in the primary and secondary somatosensory cortices (S1 & S2) across all participants (**Figure S1**). Clear somatosensory evoked responses were observed in both participants with PD and controls, with the expected SI (53 ms) and SII (132 ms) components following electrical stimulation.

We then investigated whether we could replicate the results from Andersen & Dalal (2021): [10] that neurotypical participants showed a significant increase in beta-band activity (14-30 Hz) in Cerebellum-L VI for omissions following non-jittered rhythms compared to omissions following jittered rhythms. This is also what we report here, i.e. an effect in Cerebellum-L VI, peaking at 85 ms: t_{24} = 3.98, p = 0.00056 (MNI152: x = -15.0 mm, y = -75.0 mm, z = -23.0 mm) (**Figure 2**). A cluster permutation test for the peak source in the Cerebellum-L VI for controls showed a significant difference between the omissions following non-jittered rhythms and omissions following jittered rhythms (p = 0.047); the cluster informing the rejection of the cluster null hypothesis extended from 69 ms to 99 ms, which is part of the time range reported in Andersen and Dalal (2021)[10]. Using an identical approach for PD participants resulted in a peak at 49 ms: t_{23} = 2.09, p = 0.0476 (MNI152: x = -30.0 mm, y = -38.0 mm, z = -38.0 mm). The cluster permutation test did not, however, reveal evidence for rejecting the null hypothesis (p = 0.438).

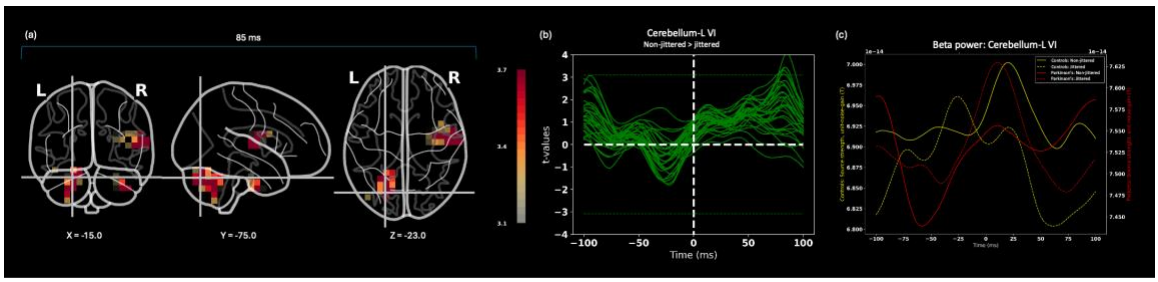

***Figure 2. Replication**. **(a)** Effect of regularity (non-jittered vs. jittered) for controls; **(b)** t-values (df=24) peaking at left cerebellum VI at t = 83 ms, similar to earlier studies [12,21] – thresholded at critical t-value for p=0.005 for controls. The lines in the panel indicate averages for the sources in the region of interest, not subjects. (c) the raw beta values for controls and participants with PD for the jittered and non-jittered conditions.*

When plotting the interaction (**Figure 3a**), a significant peak was revealed in the time range from –100 ms to 100 ms in Cerebellum-L Crus I (cerebellar ROI) (MNI152: x = -52.5 mm, y = -67.5 mm, z = -37.5 mm; t = -23 ms), $F_{1,48}$ = 12.0, p = 0.0011 (**Figure 3b**), and in Caudate-L (basal ganglia ROI) (MNI152: x = -15.0 mm, y = 15.0 mm, z = 0.0 mm; t = -14 ms), $F_{1,48}$ = 19.5, p = 0.000056 (**Figure 3c**). The cluster permutation test for

the peak source in the Cerebellum-L Crus I showed a significant difference between the controls and participants with PD (p = 0.016); the cluster informing the rejection of the cluster null hypothesis extended from –41 ms to 0 ms. A similar significant difference was found for the Caudate-L (p < 0.005); the cluster informing the rejection of the cluster null hypothesis extended from –36 ms to 5 ms.

When testing for the direction of the interaction for the Cerebellum-L Crus I (t=-23 ms), we found that controls responded more strongly to the jittered omissions than to the non-jittered omissions, t_{24} = -2.22, p = 0.036, whereas the opposite pattern was found for participants with PD, t_{23} = 2.67, p = 0.014.

When testing for the direction of the interaction for Caudate-L (t = -14 ms), we found that controls responded more strongly to the non-jittered omissions than to the jittered omissions, t_{24} = 2.96, p = 0.0068, whereas the opposite pattern was found for participants with PD, t_{23} = -3.26, p = 0.0034**.**

To test the link between PD related symptoms and the reported interaction in the cerebellum (r = 0.452, p = 0.0267) (**Figure 3f**) and the basal ganglia (r = 0.287, p = 0.174) (**Figure 3g**), we calculated the partial correlation between the peak ratio difference, at –23 ms and –14 ms respectively, for each PD participant with the UPDRS-III score, after regressing out age.

In summary, our results indicate that Cerebellum-L IV shows differential beta-band activity to omissions following respectively non-jittered and jittered rhythms in controls for the peak at 85 ms *after* the expected, but omitted, stimulus, similar to what has been reported before [10,]. In contrast, *before* the expected, but omitted, stimulus, basal ganglia (Caudate-L) (-14 ms) and Cerebellum-L Crus I (-23 ms) beta-band activity differ between group (PD vs controls) and regularity (non-jittered vs jittered), indicating altered timing mechanisms in PD. Note that the different absolute levels of beta band activity between controls and PD participants (**Figure 3d** and **Figure 3e**), have no bearing on the interactions presented here, as between-group differences are controlled for by using the ratio between non-jittered and jittered omissions to estimate the effect of regularity.

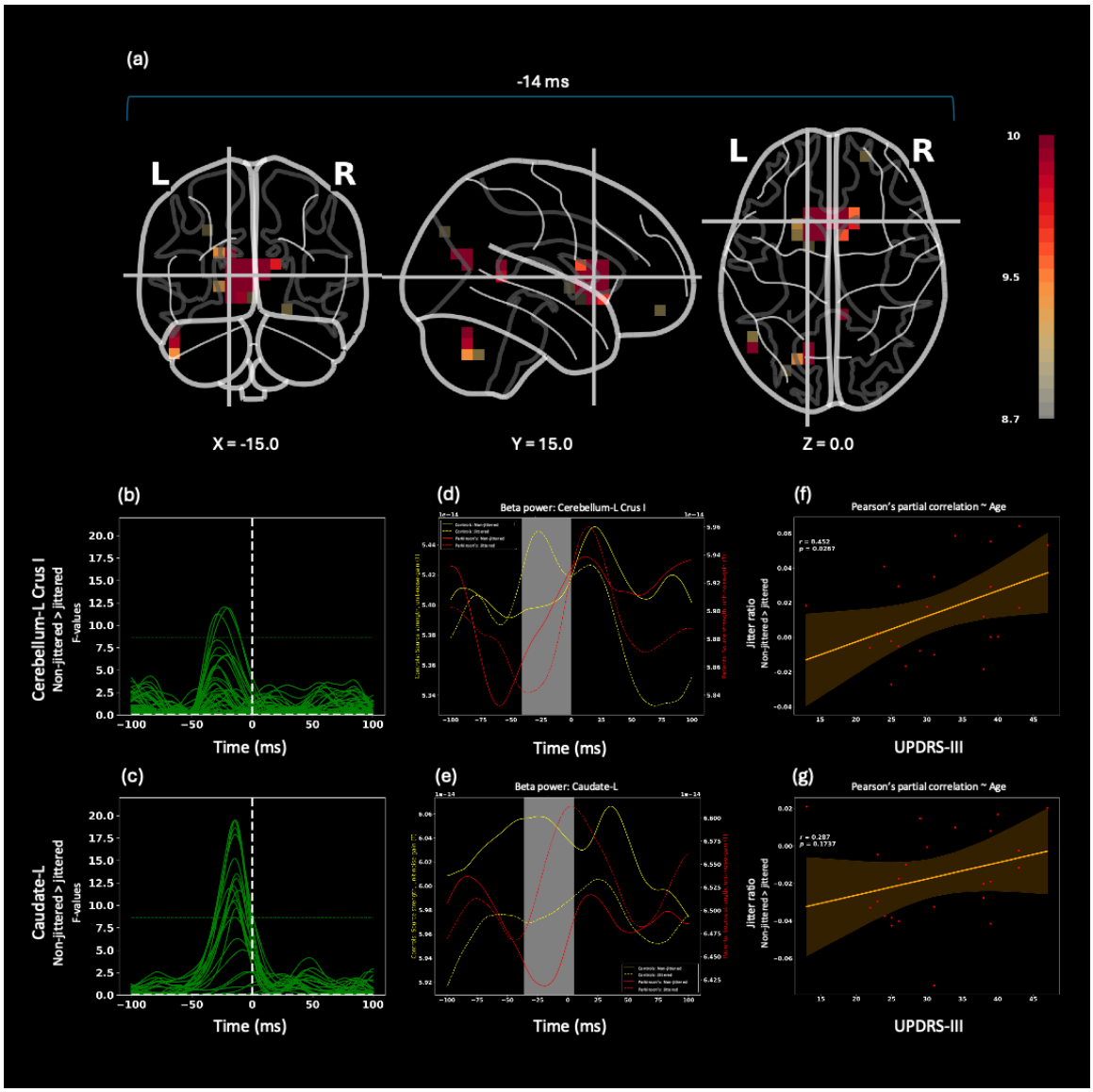

Figure 3. Interaction *between group (PD vs controls) and regularity (non-jittered vs jittered)****. (a)*** *Thresholded at p=0.005 at t = –14 ms. Color shows F-values. Of note are the caudate and cerebellar findings.* ***(b)*** *An interaction in Cerebellar-L Crus I, peaking at –23 ms.* ***(c)*** *An interaction in Caudate-L, peaking at –14 ms. The lines in panels b and c indicate averages for the sources in the region of interest, not subjects.* ***(d)****: Cerebellum-L Crus I average beta activity: in controls, beta-band activity is higher in the jittered condition than in the non-jittered condition. Participants with PD show the opposite pattern.* ***(e)****: Caudate-L average beta activity: in controls, beta-band activity is higher in the non-jittered condition than in the jittered condition. Participants with PD show the opposite pattern. The grey boxes indicate the regions informing the rejection of the cluster null hypothesis. Also note that there are separate y-axes for healthy controls and PD participants* ***Partial correlations*** *between UPDRS-III scores and the ratio between non-jittered and jittered beta-band activity for the maximum source peaking (****f****) at peak time (-23 ms) for Cerebellum-L Crus I and (****g****) at peak time (-14 ms) for Caudate-L. Shaded areas are 95 % prediction intervals. Age has been regressed out.*

To explore, whether the envelope analysis supported an interaction between Group and Regularity, we chose Caudate-L as a seed and included bilaterally, the cerebellar regions found in the current analysis (Cerebellum-L VI and Cerebellar-L Crus I) and the regions specified in earlier work (Motor Cortex and Thalamus and Caudate) [17]. This was, in part, motivated by the descriptive plot (**Figure 4a**) showing that the greatest differences were connections involving the caudate, and, in part, motivated by the *a priori* knowledge that the basal ganglia should be involved due to PD. By running an ANOVA testing for the interaction between Group and Regularity while controlling for Region of Interest (10 levels), we found the following significant interaction: $F_{1,967} = 4.79$, $p = 0.0289$ **(Figure 4b).**

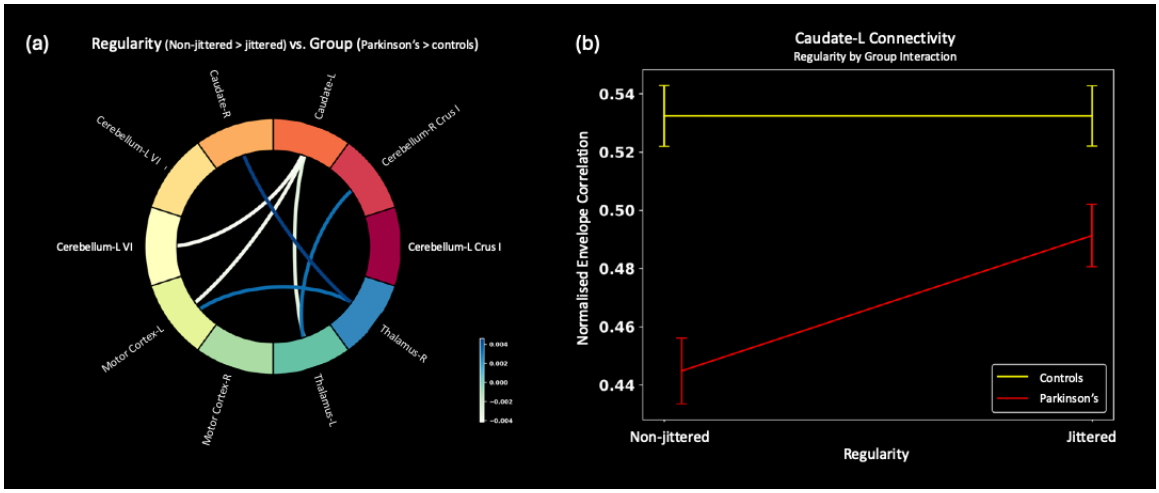

Figure 4. Functional Connectivity. *Envelope correlation findings:* ***(a)*** *all-to-all differences in connectivity between regions of interest, thresholded to show only the 6 greatest differences (the minimum number of connections required to reveal all functional links to the proposed network [17] involving the left caudate). Left caudate shows differences to all regions of the proposed network, i.e. cerebellum, thalamus and the motor cortex.* ***(b)*** *Group by Regularity interaction for the connections that involve left caudate. Participants with PD show higher connectivity during the jittered condition than during the non-jittered condition. Error bars are standard errors of the mean.*

3. Discussion

Summary of Key Findings

This study investigated cerebellar and basal ganglia beta-band (14-30 Hz) activity in participants with PD compared to controls during a rhythmic somatosensory timing task. Our findings revealed that:

1. *After* the expected but omitted stimulus (85 ms), the cerebellum reacted more strongly to omissions following non-jittered than jittered rhythms for controls.
2. *Before* the expected but omitted stimulus, the group and regularity factors interacted in a non-linear manner for the basal ganglia (-14 ms) and the cerebellum (-23 ms).
3. Cerebellar activity (-23 ms) correlated with symptom severity (UPDRS-III) in participants with PD.
4. Participants with PD showed an increase in functional connectivity for the jittered relative to the non-jittered rhythms.

Explication of interactions

To clarify the group interactions, we first consider the control group. Consistent with theories of rhythmic cognition, the basal ganglia showed stronger responses to non-jittered rhythms, as shown by prior functional magnetic resonance imaging (fMRI) studies [11,36].

In terms of the cerebellar activity *before* the expected stimulus, i.e. that beta-band power is greater following jittered rhythms than following non-jittered rhythms, it is likely that the cerebellum shows less activity for the non-jittered rhythms, as the timing of the upcoming, expected, but omitted, stimulus is highly predictable. This aligns with findings that the cerebellum responds more strongly to non-beat or irregular rhythms, while the basal ganglia prefer beat-based, regular input [11,16].

In PD, this pattern was reversed. The basal ganglia showed stronger responses to jittered rhythms, possibly reflecting compensatory effort to extract rhythmicity in the absence of clear timing cues—consistent with prior work showing greater basal ganglia activation when internally generating a beat [11]. Conversely, the cerebellum in PD showed stronger responses to non-jittered rhythms, suggesting a compensatory mechanism: when basal ganglia fail to label regular input as beat-based, the cerebellum steps in, consistent with its preference for processing non-beat rhythms.

Cerebellum and temporal processing: *Evaluation* vs. *Prediction*

Our findings indicate that the cerebellum displays a beta-band response peaking at 85 ms *after* the omitted stimulus in controls. This result replicates earlier findings [10] and aligns with the proposal by Andersen & Dalal (2024b) [17] that the cerebellum is not directly responsible for timing functions but plays a key role in integrating sensory predictions with sensory feedback.

However, the observed differences in cerebellum crus I *before* the omitted stimulus suggest that, while the cerebellum may not be directly involved in beat-based timing in the otherwise healthy brain, it may play a compensatory role in PD. This is supported by the correlation between symptom severity and the magnitude of the cerebellar responses to non-jittered versus jittered omissions.

Our findings contribute to a growing body of literature suggesting that the cerebellum plays a role in building sensory predictions rather than directly controlling the timing of sensory events. The observed differences in cerebellar regions in participants with PD *before* the omitted stimulus indicate potential compensatory mechanisms that are disrupted in the disease, underscoring the cerebellum's broader role in temporal prediction and motor control.

It should be noted that the seventh event was never globally expected, as each stimulation train consisted of six pulses. However, prior work has shown that omissions can generate cerebellar responses even when they are not globally expected, provided they are locally predictable within a train [12,13,21]. Our paradigm thus probes local temporal predictions rather than global sequence expectations, consistent with the replicated cerebellar omission responses reported here.

Basal Ganglia Dysfunction and Altered Timing Mechanisms in Parkinson's disease

The significant alteration in beta-band activity in the caudate nucleus between participants with PD and controls underscores the basal ganglia's pivotal role in temporal processing. The basal ganglia, particularly the caudate and putamen, have long been implicated in the regulation of motor control and timing [9]. Our findings are consistent with a large body of literature showing that PD impairs both motor and perceptual timing tasks. Notably, the basal ganglia dysfunction plays a central role in these deficits [29].

Beta-band activity within the basal ganglia is thought to maintain the current motor state and suppress voluntary movements until the appropriate time for action [37]. This rhythmic activity is crucial for the fine-tuning of temporal predictions and the execution of time-sensitive motor behaviors [38]. The different beta-band responses observed in PD suggest a failure in the basal ganglia's ability to appropriately modulate these timing signals.

Furthermore, neuroimaging studies have demonstrated that the basal ganglia are critical for interval timing and the perception of temporal sequences [28,39,40]. These studies indicate that the caudate nucleus is particularly involved in the processing of temporal expectations and the updating of internal models based on sensory feedback. Our findings extend this understanding by showing that participants with PD exhibit altered beta-band activity in the caudate during tasks requiring precise temporal predictions, suggesting a diminished capacity to adjust timing based on sensory input.

Beta-Band Connectivity between Basal Ganglia and Cerebellum, Thalamus and Motor Cortex

We find evidence that the connectivity in the beta-band between the caudate and cerebellum, thalamus and motor cortex specifically changes for PD. Compared to controls, participants with PD showed an increase in connectivity for the jittered condition compared to the non-jittered condition. Similarly, in PD we found that the caudate reacted more strongly to the jittered stimuli than the non-jittered stimuli. These increases may reflect the underlying network (basal ganglia, cerebellum, thalamus and motor cortex) synchronizing more tightly to integrate timing information with action plans [21]. In other words, the network is 'trying harder' to generate an internal beat to interpret the jittered sequence as rhythmic [11].

Our connectivity findings also align with extensive work on motor cortical beta oscillations. Motor cortex beta activity is thought to maintain the current motor set and inhibit premature actions, with transient beta suppression enabling movement initiation [37,38]. In PD, exaggerated beta synchrony between motor cortex and basal ganglia is a well-documented pathophysiological hallmark [41], and is attenuated by dopaminergic therapy or deep brain stimulation. In our study, participants with PD showed an increase in connectivity during the jittered condition relative to the non-jittered condition. We interpret this increase as potentially reflecting the same pathophysiological mechanism of excessive beta synchrony, but here manifesting in a context where the network relies on additional resources to impose regularity on irregular input. Thus, the altered connectivity we observe between caudate, cerebellum, thalamus and motor cortex likely reflects disruptions in this wider beta-band network, consistent with both cortical and subcortical contributions to impaired temporal prediction and motor control in PD. The seeming difference in connectivity between the two groups may be driven by controls in general showing higher beta band activity than PD participants (**Figure 3d** and **Figure3e**) [42]. However, this is not an issue for the interpretation of the interaction, which is independent of average differences between groups.

Limitations

One limitation concerns the participant sample, while comparable to similar neurophysiological studies, we may have limited statistical power for detecting smaller effect sizes. Our study included only medicated participants with PD, which means that the effects of dopaminergic medication on beta-band activity cannot be ruled out.

Another limitation is that despite MEG being a powerful tool for investigating neural activity with high temporal resolution, it has limited sensitivity to central brain structures, such as the basal ganglia. This limitation is mitigated by the observation that our magnetoencephalographic basal ganglia findings in controls concord with what is found in functional magnetic resonance imaging studies [11,16,36,40], namely that the basal ganglia preferentially respond to non-jittered stimuli. It is furthermore mitigated by the *a priori* knowledge that this is exactly where participants with PD should show dysfunctional activity, which is precisely what our results show. Finally, as we relied on omissions to elicit activity, cortical activity of the cerebrum, which might otherwise mask sub-cortical activity, was kept to a minimum [32].

An important consideration concerns the lateralization of our findings. The most robust source-level effects emerged in the left cerebellum and left basal ganglia, despite the well-documented contralateral connectivity of the cerebello–cortico–striatal system (i.e., left cerebellum to right basal ganglia and motor cortex). Several factors may contribute: (i) tactile stimulation was delivered to the right index finger, favoring contralateral (left-hemisphere) responses; (ii) all participants were right-handed, consistent with left-dominant sensorimotor processing; and (iii) MEG beamforming sensitivity can differ across hemispheres. Importantly, functional asymmetries in cerebellar and basal ganglia activation during timing tasks have been reported previously [10,24,47,48], suggesting that lateralized effects are not unusual. At the connectivity level, we additionally observed coupling between the left basal ganglia and right cerebellum (**Figure 4**), consistent with cross-hemispheric cerebello–striatal loops. Taken together, the apparent "left–left" effects may therefore reflect both methodological sensitivity and known asymmetries, but our sample was not stratified by side of symptom onset in PD, so we cannot directly relate lateralization to clinical laterality. Future work with larger and side-stratified samples may clarify this issue.

Finally, the groups were not gender-matched, and controls were only age-matched at the group level rather than individually paired. While these discrepancies are common in MEG/PD studies, they may nonetheless have influenced the results and should be considered when generalizing our findings.

Conclusion

In conclusion, the cerebellum shows preserved evaluative beta-band responses in PD, while basal ganglia dysfunction alters predictive timing signals. Increased cerebellar activity before predicted stimuli, correlating with symptom severity, suggests a compensatory role. PD also disrupts connectivity within a sensory-integration network involving the cerebellum, basal ganglia, thalamus and primary motor cortex.

These findings extend beyond clinical characterization of PD: they provide mechanistic insight into how rhythmic cognition emerges from the interplay between predictive and evaluative processes in subcortical–cortical networks. Beta-band oscillations in the cerebello–striatal–thalamo–cortical circuit support temporal prediction during regular rhythms and evaluation when these predictions are violated. PD reveals how perturbing basal ganglia function shifts this balance, increasing reliance on cerebellar engagement and altering network connectivity, particularly under irregular rhythmic conditions.

By combining high-temporal-resolution MEG with a rhythmic omission paradigm, we identify key neural signatures of predictive timing and their reorganization in PD. This work bridges basic rhythmic cognition research and clinical neuroscience, offering a network-level framework to interpret timing dysfunction and pointing to potential rhythm-based biomarkers and therapeutic targets.

4. Materials and Methods

Participants

Participants in the study were individuals diagnosed with PD as well as an age-matched control group without PD, henceforth "controls". All participants in the study were right-handed. The study was approved by the regional ethics committee (De Videnskabsetiske Komitéer for Region Midtjylland) in accordance with the Declaration of Helsinki. Participants were recruited following ethical guidelines and provided informed consent before participating in the study.

Detailed demographic information was recorded for each participant (**Table 1**). Groups were age-matched at the group level, with mean ages differing by ~6 years (controls: 60.2 ± 9.4 years; PD: 66.0 ± 7.8 years), but not individually paired by age. Gender distribution was not matched, with a higher proportion of females in the control group. Participants were screened for mild cognitive impairment using the Montreal Cognitive Assessment (MoCA) [54] and depression symptoms using the Major Depression Inventory (MDI) [55] and were excluded if they scored less than 26 and higher than 24, respectively. None were excluded based on these scores.

To assess the severity of PD, the motor examination of the Movement Disorder Society's Unified Parkinson's Disease Rating Scale (UPDRS-III) [56] was performed by the team physicians. Participants with PD were asked to take their daily medication as normal, without interruption (**Figure S2, Table S1**). Fifty-six participants were recruited for the project. Of these, 3 had metal plates in their body that disturbed MEG recordings, 3 were revealed to be left-handed, and one had atrophy in the cerebellum, resulting in a final sample of 49 participants.

Stimuli and Procedure

Tactile stimulation was administered using two ring electrodes powered by an electric current generator (Stimulus Current Generator, DeMeTec GmbH, Germany). These ring electrodes were affixed to the tip of the right index finger, with one placed 10 mm below the bottom of the nail and the other 10 mm below that.

Stimuli were delivered using PsychoPy (version 3.2.4) [57] on a Linux operating system running Ubuntu Mate (kernel version 4.15.0-126). Six short breaks were administered throughout the session to ensure participant comfort and to verify their well-being through verbal communication with the experimenter.

Stimuli were presented in sequences of six, with an inter-stimulus interval of 1,497 ms to prevent synchronization with the 50 Hz power line interference. Each pulse had a duration of 100 µs, and the level of current was individually adjusted for each participant. In each sequence, the sixth stimulus was followed by an omission, marking the start of a new stimulation train. Thus, a 2,994 ms interval elapsed between the last stimulus of one train and the first stimulus of the next. Three types of sequences were administered (**Figure 1**):

1. Non-Jittered Somatosensory Rhythms: All stimuli occurred precisely on time (0% jitter).
2. Jittered Somatosensory Rhythms: Stimuli 4–6 were jittered by 15%, occurring from -225 ms to +225 ms relative to the non-jittered sequence. The jitter administered on a given stimulus is drawn from a uniform distribution in steps of 1 ms.
3. Non-Stimulation Sequence: A train of seven non-stimulations, each lasting 1,497 ms, occurred after every fifteen stimulation sequences.

Each stimulation sequence type was administered 150 times, while the non-stimulation sequence was administered 30 times. The sequences were pseudorandomly interleaved and counterbalanced to mitigate order effects. Participants were instructed to watch a nature program with sound from panel

speakers during the stimulation procedure and were instructed to focus on the center of the screen, remain motionless, and disregard the finger stimulation. The non-stimulation sequences were not further analyzed.

Preparation of Participants

Participants underwent standard MEG preparation, including Electrooculography (EOG), electrocardiography (ECG), electromyography (EMG), and respiration recordings to monitor eye movements, cardiac activity, muscle tension and breathing. EOG electrodes were placed around the eyes, ECG on the collarbones, and EMG on the splenius muscles. Four HPI coils were attached to the head, and head shape digitization was performed using Polhemus FASTRAK, including fiducials and ~200 extra points. Participants were positioned supine in the MEG scanner with ring electrodes secured to the right index finger. Stimulation current was individually adjusted: starting at 1.0 mA, increased until perceptible but not irritating, and then fine-tuned for comfort.

Data Acquisition

Data was acquired at Aarhus University Hospital (AUH), Denmark. MEG data was acquired using an Elekta Neuromag TRIUX system located within a magnetically shielded room (Vacuumschmelze Ak3b). The sampling frequency was 1,000 Hz; online filtering was applied to the acquired data, consisting of a low-pass filter with a cutoff frequency of 330 Hz and a high-pass filter with a cutoff frequency of 0.1 Hz.

MEG Data Processing

MEG data were processed using MNE-Python [56] following Andersen (2018) [59]. Bad channels (mean = 0.22 per participant) were excluded based on power spectra inspection. For evoked responses, data were low-pass filtered at 40 Hz [one-pass, noncausal, finite impulse response; zero phase; upper transition bandwidth: 10.00 Hz (−6 dB cutoff frequency: 45.00 Hz; filter length 331 samples; a 0.0194 passband ripple and 53 dB stopband attenuation)], epoched (−200 to 600 ms), baseline-corrected (-100 ms – 0 ms(, and averaged by condition. Beta-band responses (14–30 Hz) were extracted by band-pass filtering [14–30 Hz; lower transition bandwidth: 3.50 Hz (−6 dB cutoff frequency: 12.25 Hz); upper transition bandwidth: 7.50 Hz (−6 dB cutoff frequency: 33.75 Hz); filter length 943 samples; passband ripple: 0.0194; stopband attenuation: 53 dB)], Hilbert transforming, and epoching from −750 to +750 ms around each stimulus or omission (baseline correct (-750 ms to 750 ms). Since we were concerned with the difference in ratios (non-jittered vs jittered) between the groups (controls vs PD), any absolute differences in beta band activity were controlled for. The main analysis of interest was the beta band activity. Evoked responses were extracted to do sanity checks of whether SI and SII components were elicited (Figure S1).

Source Reconstruction

Neural source activity was then estimated for evoked responses and average beta band activity using beamforming to achieve high spatial resolution. Each participant underwent structural MRI (Siemens Magnetom Prisma 3T, 1 mm isotropic MPRAGE). The pulse sequence parameters were as follows: 1 mm isotropic resolution; field of view, 256 × 240 mm; 192 slices; slice thickness, 1 mm; bandwidth per pixel, 290 Hz/pixel; flip angle, 9°; inversion time (TI), 1,100 ms; echo time (TE), 2.61 ms; and repetition time (TR), 2,300 ms. We furthermore acquired T2-weighted 3D images. The pulse sequence parameters were as follows: 1 mm isotropic resolution; field of view, 256 × 240 mm; 96 slices; slice thickness, 1.1 mm; bandwidth per pixel, 780 Hz/pixel; flip angle, 111°; echo time, 85 ms; and repetition time, 14,630 ms. These images were processed with FreeSurfer [60,61] to segment the head and brain surfaces. A volumetric source space (~4,000 sources, 7.5 mm spacing) was generated using MNE-C's watershed algorithm [62]. Single compartment boundary element method (BEM) models were constructed, and MRI–MEG co-

registration was performed using Polhemus FASTRAK fiducials and head shape points. Forward models were computed from co-registered data.

Source estimation used a linearly constrained minimum variance (LCMV) beamformer [63] with the unit-noise-gain constraint, applied separately to evoked and beta-band data. The data covariance matrices were estimated from post-stimulus periods for the evoked responses and for the full epoch for the beta-band responses and used without regularization due to good conditioning of the covariance matrices. Magnetometer data were used for optimal sensitivity to deep sources.

Statistical Analysis

Statistical analyses focused on identifying significant differences in beta-band responses between the ratios of the two omission conditions (non-jittered and jittered) in source space. Regions of interest were chosen based on previous experiments [12,21] and theory [17]. The regions of interest were the left cerebellum crus I and left cerebellum VI, where we have found expectation related effects between non-jittered and jittered omissions in earlier studies [12,21] and the basal ganglia, here taken to be the caudate, the putamen and the pallidum (both hemispheres) [17].

Statistical maps for omissions were plotted for these regions, showcasing the interaction between Group (PD and controls) and Regularity (non-jittered and jittered), as these highlight where there are differences between the two groups in terms of how they build expectations under ideal (non-jittered) and less than ideal (jittered) conditions. The time range of interest was chosen to be from 100 ms before the expected stimulus to 100 ms after the expected stimulus. The difference between the non-jittered and the jittered conditions were calculated as the following ratio: $\frac{(x_1 - x_2)}{(x_1 + x_2)}$

For each of the two regions of interest (the cerebellum and the basal ganglia), we identified the source with the peak value for the interaction in the range from –100 ms to 100 ms. To control the false alarm rate for the time dimension, we applied cluster permutation analyses [64] over the time courses for the maximal sources in the cerebellum and the basal ganglia using 1024 permutations.

To examine the relationship between neural activity and clinical severity, we computed partial correlations between beta-band activity and UPDRS-III scores within the PD group. Specifically, we calculated the ratio difference in beta power between non-jittered and jittered omissions at the peak latencies of –23 ms (cerebellum) and –14 ms (caudate) and tested their association with UPDRS-III motor scores. Age was included as a covariate, as it is known to influence both neural oscillatory dynamics and motor performance in PD and may otherwise confound symptom–brain associations [65–67].

Envelope correlations

To test functional connectivity between regions of interest, we used envelope correlation [68]. We investigated the envelope correlations in the beta-band from –100 ms to 100 ms the omitted stimulation. Regions of interest were based on the proposed network of sensory prediction from Andersen & Dalal (2024b) [17], which is constituted of basal ganglia, thalamus, cerebellum and the primary motor cortex. We included these areas bilaterally – and explored the functional connectivity within this proposed network. For descriptive purposes, we estimated the all-to-all connectivity between these nodes.

Author Contributions:

VPN: Investigation, Writing – Original Draft, Writing – Review & Editing, Visualization.

LMA: Conceptualization, Methodology, Software, Validation, Formal Analysis, Investigation, Data Curation, Writing – Original Draft, Writing – Review & Editing, Visualization, Supervision, Project Administration, Funding Acquisition.

Financial Disclosures of all authors (for the preceding 12 months):

V.P.N. is funded by the Center for Music in the Brain (MIB), supported by the Danish National Research Foundation (DNRF 117). L.M.A. was funded by the Lundbeck Foundation (R322-2019-1841). The funders had no role in study design, data collection and analysis, decision to publish, or preparation of the manuscript. The authors declare that there are no conflicts of interest relevant to this work, and that there are no additional disclosures to report.

Data sharing:

The raw MRI data underlying this study contain sensitive personal information and cannot be fully shared publicly due to restrictions imposed by the General Data Protection Regulation (GDPR) and Danish national data protection laws. However, analysis scripts and code used for data processing and visualization are available at (https://github.com/ualsbombe/pd_cerebellum). Requests for access to the raw MRI data can be submitted to the corresponding author and will require a formal data-sharing agreement and approval from the relevant parties. The raw MEG data will be shared upon reasonable request to the corresponding author.

References

1. Blakemore, S.-J., Wolpert, D. M. & Frith, C. D. Central cancellation of self-produced tickle sensation. *Nat. Neurosci.* **1**, 635–640 (1998).
2. Clark, A. Whatever next? Predictive brains, situated agents, and the future of cognitive science. *Behav. Brain Sci.* **36**, 181–204 (2013).
3. Gross, J. *et al.* The neural basis of intermittent motor control in humans. *Proc. Natl. Acad. Sci.* **99**, 2299–2302 (2002).
4. Miall, R. C., Weir, D. J., Wolpert, D. M. & Stein, J. F. Is the cerebellum a smith predictor? *J. Mot. Behav.* **25**, 203–216 (1993).
5. Wolpert, D. M. & Kawato, M. Multiple paired forward and inverse models for motor control. *Neural Netw. Off. J. Int. Neural Netw. Soc.* **11**, 1317–1329 (1998).
6. Schmahmann, J. D. & Pandya, D. N. The cerebrocerebellar system. *Int. Rev. Neurobiol.* **41**, 31–60 (1997).
7. Kakei, S. *et al.* Contribution of the Cerebellum to Predictive Motor Control and Its Evaluation in Ataxic Patients. *Front. Hum. Neurosci.* **13**, (2019).
8. Peterburs, J. & Desmond, J. E. The role of the human cerebellum in performance monitoring. *Curr. Opin. Neurobiol.* **40**, 38–44 (2016).
9. Coull, J. T., Hwang, H. J., Leyton, M. & Dagher, A. Dopamine Precursor Depletion Impairs Timing in Healthy Volunteers by Attenuating Activity in Putamen and Supplementary Motor Area. *J. Neurosci.* **32**, 16704–16715 (2012).
10. Grahn, J. A. & Brett, M. Rhythm and beat perception in motor areas of the brain. *J. Cogn. Neurosci.* **19**, 893–906 (2007).
11. Grahn, J. A. & Rowe, J. B. Feeling the beat: Premotor and striatal interactions in musicians and nonmusicians during beat perception. *J. Neurosci.* **29**, 7540–7548 (2009).
12. Andersen, L. M. & Dalal, S. S. The cerebellar clock: Predicting and timing somatosensory touch. *NeuroImage* **238**, 118202 (2021).
13. Tesche, C. D. & Karhu, J. J. T. Anticipatory cerebellar responses during somatosensory omission in man. *Hum. Brain Mapp.* **9**, 119–142 (2000).
14. Buhusi, C. V. & Meck, W. H. What makes us tick? Functional and neural mechanisms of interval timing. *Nat. Rev. Neurosci.* **6**, 755–765 (2005).
15. Grube, M., Cooper, F. E., Chinnery, P. F. & Griffiths, T. D. Dissociation of duration-based and beat-based auditory timing in cerebellar degeneration. *Proc. Natl. Acad. Sci. U. S. A.* **107**, 11597–11601 (2010).
16. Teki, S., Grube, M., Kumar, S. & Griffiths, T. D. Distinct Neural Substrates of Duration-Based and Beat-Based Auditory Timing. *J. Neurosci.* **31**, 3805–3812 (2011).
17. Andersen, L. M. & Dalal, S. S. The role of the cerebellum in timing. *Curr. Opin. Behav. Sci.* **59**, 101427 (2024).
18. Criscuolo, A., Schwartze, M., Nozaradan, S. & Kotz, S. A. Basal ganglia and cerebellar lesions causally impact the neural encoding of temporal regularities. *Imaging Neurosci.* **3**, imag_a_00492 (2025).
19. Caligiore, D. *et al.* Parkinson's disease as a system-level disorder. *NPJ Park. Dis.* **2**, 16025 (2016).
20. Grahn, J. A. & Brett, M. Impairment of beat-based rhythm discrimination in Parkinson's disease. *Cortex* **45**, 54–61 (2009).
21. Andersen, L. M. & Dalal, S. S. Detection of Threshold-Level Stimuli Modulated by Temporal Predictions of the Cerebellum. *eneuro* **11**, ENEURO.0070-24.2024 (2024).

22. Arnal, L. H. Predicting “When” Using the Motor System’s Beta-Band Oscillations. *Front. Hum. Neurosci.* **6**, (2012).
23. Te Woerd, E. S., Oostenveld, R., Bloem, B. R., De Lange, F. P. & Praamstra, P. Effects of rhythmic stimulus presentation on oscillatory brain activity: The physiology of cueing in Parkinson’s disease. *NeuroImage Clin.* **9**, 300–309 (2015).
24. Vinding, M. C. *et al.* Attenuated beta rebound to proprioceptive afferent feedback in Parkinson’s disease. *Sci. Rep.* **9**, 2604 (2019).
25. Vinding, M. C. *et al.* Oscillatory and non-oscillatory features of the magnetoencephalic sensorimotor rhythm in Parkinson’s disease. *Npj Park. Dis.* **10**, 1–13 (2024).
26. DeLong, M. R. & Wichmann, T. Circuits and circuit disorders of the basal ganglia. *Arch. Neurol.* **64**, 20–24 (2007).
27. Kalia, L. V. & Lang, A. E. Parkinson’s disease. *Lancet Lond. Engl.* **386**, 896–912 (2015).
28. Jones, C. R. G. & Jahanshahi, M. Motor and Perceptual Timing in Parkinson’s Disease. in *Neurobiology of Interval Timing* (eds Merchant, H. & de Lafuente, V.) 265–290 (Springer, New York, NY, 2014). doi:10.1007/978-1-4939-1782-2_14.
29. Harrington, D. L. *et al.* Neurobehavioral Mechanisms of Temporal Processing Deficits in Parkinson’s Disease. *PLOS ONE* **6**, e17461 (2011).
30. Andersen, L. M., Jerbi, K. & Dalal, S. S. Can EEG and MEG detect signals from the human cerebellum? *NeuroImage* **215**, 116817 (2020).
31. Samuelsson, J. G., Sundaram, P., Khan, S., Sereno, M. I. & Hämäläinen, M. S. Detectability of cerebellar activity with magnetoencephalography and electroencephalography. *Hum. Brain Mapp.* **41**, 2357–2372 (2020).
32. Krishnaswamy, P. *et al.* Sparsity enables estimation of both subcortical and cortical activity from MEG and EEG. *Proc. Natl. Acad. Sci.* **114**, E10465–E10474 (2017).
33. Attal, Y., Maess, B., Friederici, A. & David, O. Head models and dynamic causal modeling of subcortical activity using magnetoencephalographic/electroencephalographic data. **23**, 85–95 (2012).
34. Fujioka, T., Trainor, L. J., Large, E. W. & Ross, B. Internalized Timing of Isochronous Sounds Is Represented in Neuromagnetic Beta Oscillations. *J. Neurosci.* **32**, 1791–1802 (2012).
35. Piastra, M. C. *et al.* A comprehensive study on electroencephalography and magnetoencephalography sensitivity to cortical and subcortical sources. *Hum. Brain Mapp.* **42**, 978–992 (2021).
36. Grahn, J. A. & Rowe, J. B. Finding and feeling the musical beat: Striatal dissociations between detection and prediction of regularity. *Cereb. Cortex* **23**, 913–921 (2013).
37. Engel, A. K. & Fries, P. Beta-band oscillations--signalling the status quo? *Curr. Opin. Neurobiol.* **20**, 156–165 (2010).
38. Jenkinson, N. & Brown, P. New insights into the relationship between dopamine, beta oscillations and motor function. *Trends Neurosci.* **34**, 611–618 (2011).
39. Jones, C. R. G. & Jahanshahi, M. Contributions of the Basal Ganglia to Temporal Processing: Evidence from Parkinson’s Disease. *Timing Time Percept.* **2**, 87–127 (2014).
40. Rao, S. M., Mayer, A. R. & Harrington, D. L. The evolution of brain activation during temporal processing. *Nat. Neurosci.* **4**, 317–323 (2001).
41. Kühn, A. A., Kupsch, A., Schneider, G.-H. & Brown, P. Reduction in subthalamic 8–35 Hz oscillatory activity correlates with clinical improvement in Parkinson’s disease. *Eur. J. Neurosci.* **23**, 1956–1960 (2006).

42. Bastos, A. M. & Schoffelen, J.-M. A Tutorial Review of Functional Connectivity Analysis Methods and Their Interpretational Pitfalls. *Front. Syst. Neurosci.* **9**, (2016).
43. Friston, K. A theory of cortical responses. *Philos. Trans. R. Soc. Lond. B. Biol. Sci.* **360**, 815–836 (2005).
44. Fujioka, T., Trainor, L. J., Large, E. W. & Ross, B. Internalized Timing of Isochronous Sounds Is Represented in Neuromagnetic Beta Oscillations. *J. Neurosci.* **32**, 1791–1802 (2012).
45. Large, E. W. & Jones, M. R. The dynamics of attending: How people track time-varying events. *Psychol. Rev.* **106**, 119–159 (1999).
46. Kühn, A. A., Kupsch, A., Schneider, G.-H. & Brown, P. Reduction in subthalamic 8-35 Hz oscillatory activity correlates with clinical improvement in Parkinson's disease. *Eur. J. Neurosci.* **23**, 1956–1960 (2006).
47. Wu, T., Hou, Y., Hallett, M., Zhang, J. & Chan, P. Lateralization of brain activity pattern during unilateral movement in Parkinson's disease. *Hum. Brain Mapp.* **36**, 1878–1891 (2015).
48. Schlerf, J. E., Galea, J. M., Spampinato, D. & Celnik, P. A. Laterality Differences in Cerebellar–Motor Cortex Connectivity. *Cereb. Cortex* **25**, 1827–1834 (2015).
49. Kotz, S. A., Ravignani, A. & Fitch, W. T. The Evolution of Rhythm Processing. *Trends Cogn. Sci.* **22**, 896–910 (2018).
50. Manto, M. *et al.* Consensus Paper: Novel Directions and Next Steps of Non-invasive Brain Stimulation of the Cerebellum in Health and Disease. *The Cerebellum* **21**, 1092–1122 (2021).
51. Pando-Naude, V., Jespersen, K. V., Johnsen, E. & Vuust, P. Rhythmic auditory stimulation for motor rehabilitation in Parkinson's disease. *Cochrane Database Syst. Rev.* **CD015759**, (2024).
52. Thaut, M. H. *et al.* Rhythmic auditory stimulation in gait training for Parkinson's disease patients. *Mov. Disord. Off. J. Mov. Disord. Soc.* **11**, 193–200 (1996).
53. Wang, L. *et al.* Effects of Rhythmic Auditory Stimulation on Gait and Motor Function in Parkinson's Disease: A Systematic Review and Meta-Analysis of Clinical Randomized Controlled Studies. *Front. Neurol.* **13**, 818559 (2022).
54. Nasreddine, Z. S. *et al.* The Montreal Cognitive Assessment, MoCA: a brief screening tool for mild cognitive impairment. *J Am Geriatr Soc* **53**, 695–699 (2005).
55. Olsen, L. R., Jensen, D. V., Noerholm, V., Martiny, K. & Bech, P. The internal and external validity of the Major Depression Inventory in measuring severity of depressive states. https://doi.org/10.1017/S0033291702006724 (2003) doi:10.1017/S0033291702006724.
56. Goetz, C. G. *et al.* Movement Disorder Society-Sponsored Revision of the Unified Parkinson's Disease Rating Scale (MDS-UPDRS): Scale Presentation and Clinimetric Testing Results. *Mov. Disord.* https://doi.org/10.1002/mds.22340 (2008) doi:10.1002/mds.22340.
57. Peirce, J. W. Generating stimuli for neuroscience using PsychoPy. *Front. Neuroinformatics* **2**, (2009).
58. Gramfort, A. *et al.* MEG and EEG data analysis with MNE-Python. *Front. Neurosci.* **7**, (2013).
59. Andersen, L. M. Group Analysis in MNE-Python of Evoked Responses from a Tactile Stimulation Paradigm: A Pipeline for Reproducibility at Every Step of Processing, Going from Individual Sensor Space Representations to an across-Group Source Space Representation. *Front. Neurosci.* **12**, (2018).
60. Dale, A. M., Fischl, B. & Sereno, M. I. Cortical surface-based analysis. I. Segmentation and surface reconstruction. *NeuroImage* **9**, 179–194 (1999).
61. Fischl, B. FreeSurfer. *NeuroImage* **62**, 774–781 (2012).

62. Gramfort, A. *et al.* MNE software for processing MEG and EEG data. *NeuroImage* **86**, 446–460 (2014).
63. Sekihara, K., Hild, K. E., Dalal, S. S. & Nagarajan, S. S. Performance of prewhitening beamforming in MEG dual experimental conditions. *IEEE Trans. Biomed. Eng.* **55**, 1112–1121 (2008).
64. Maris, E. & Oostenveld, R. Nonparametric statistical testing of EEG- and MEG-data. *J. Neurosci. Methods* **164**, 177–190 (2007).
65. Abdullah, R. *et al.* Parkinson's disease and age: The obvious but largely unexplored link. *Exp. Gerontol.* **68**, 33–38 (2015).
66. Seidler, R. D. *et al.* Motor control and aging: Links to age-related brain structural, functional, and biochemical effects. *Neurosci. Biobehav. Rev.* **34**, 721–733 (2010).
67. Levy, G. *et al.* Contribution of Aging to the Severity of Different Motor Signs in Parkinson Disease. *Arch. Neurol.* **62**, 467–472 (2005).
68. Hipp, J. F., Hawellek, D. J., Corbetta, M., Siegel, M. & Engel, A. K. Large-scale cortical correlation structure of spontaneous oscillatory activity. *Nat. Neurosci.* **15**, 884–890 (2012).

Figure Legends:

Figure 1. Experimental paradigm. (a) *Tactile stimuli were administered via ring electrodes placed on the right index finger, delivering sequences of six pulses with a duration of 100 µs and inter-stimulus interval of 1,497ms. PsychoPy controlled the stimulation, while participants watched a nature program and remained motionless. EOG, ECG, and EMG recordings were collected to monitor eye movements, heart activity, and neck muscle tension. Stimulus sequences included* ***(b)*** *non-jittered somatosensory rhythms,* ***(c)*** *jittered somatosensory rhythms (15%), and* ***(d)*** *non-stimulation sequences.* ***(e)*** *MEG was acquired during the paradigm and structural MRI was acquired another day within the next two weeks.*

Figure 2. Replication*.* ***(a)*** *Main effect of regularity (non-jittered vs. jittered) for controls;* ***(b)*** *t-values (df=24) peaking at left cerebellum VI at t = 83 ms, similar to earlier studies* [12,21] *– thresholded at critical t-value for p=0.005. the lines in the panel indicate averages for the sources in the region of interest, not subjects. (c) the raw beta values for controls and participants with PD for the jittered and non-jittered conditions.*

Figure 3. Interaction *between group (PD vs controls) and regularity (non-jittered vs jittered)****. (a)*** *Thresholded at p=0.005 at t = –14 ms. Color shows F-values. Of note are the caudate and cerebellar findings.* ***(b)*** *An interaction in Cerebellar-L Crus I, peaking at –23 ms.* ***(c)*** *An interaction in Caudate-L, peaking at –14 ms. The lines in panels b and c, indicate averages for the sources in the region of interest, not subjects.* ***(d)****: Cerebellum-L Crus I average beta activity: in controls, beta-band activity is higher in the jittered condition than in the non-jittered condition. Participants with PD show the opposite pattern.* ***(e)****: Caudate-L average beta activity: in controls, beta-band activity is higher in the non-jittered condition than in the jittered condition. Participants with PD show the opposite pattern. The grey boxes indicate the regions informing the rejection of the cluster null hypothesis. Also note that there are separate y-axes for healthy controls and PD participants* ***Partial correlations*** *between UPDRS-III scores and the ratio between non-jittered and jittered beta-band activity for the maximum source peaking (****f****) at peak time (-23 ms) for Cerebellum-L Crus I and (****g****) at peak time (-14 ms) for Caudate-L. Shaded areas are 95 % prediction intervals. Age has been regressed out.*

Figure 4*.* ***Functional Connectivity.*** *Envelope correlation findings:* ***(a)*** *all-to-all differences in connectivity between regions of interest, thresholded to show only the 6 greatest differences (the minimum number of connections required to reveal all functional links to the proposed network* [17] *involving the left caudate). Left caudate shows differences to all regions of the proposed network, i.e. cerebellum, thalamus and the motor cortex.* ***(b)*** *Group by Regularity interaction for the connections that involve left caudate. Participants with PD show higher connectivity during the jittered condition than during the non-jittered condition. Error bars are standard errors of the mean.*

Figure S1. Somatosensory responses *for SI (53 ms) and SII (132 ms);* ***(a)*** *Controls, n=25;* ***(b)*** *Parkinson's disease, n=24. Signal Space Projection (first four SSPs) was applied to reduce environmental noise.*

Figure S2*. Distribution of prescribed medication for Parkinson's disease symptoms. L-DOPA, levodopa; D-AGONIST, dopamine agonist; MAOI, monoamine oxidase inhibitor.*

Supplementary Information

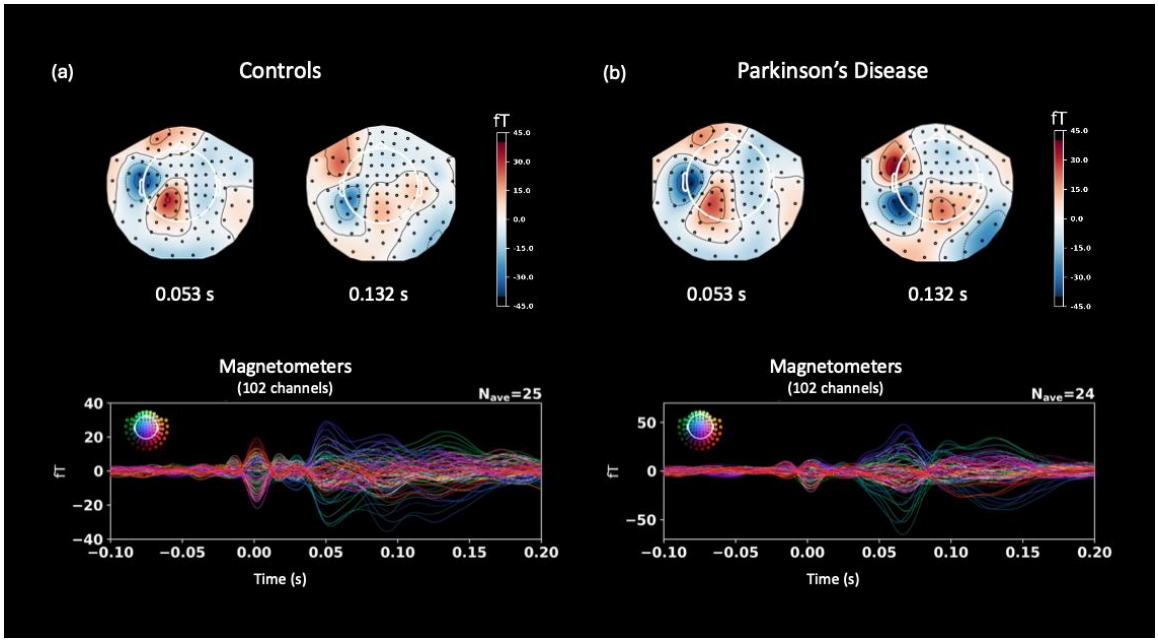

Figure S1. Somatosensory responses *for SI (53 ms) and SII (132 ms);* ***(a)*** *Controls, n=25;* ***(b)*** *Parkinson's disease, n=24. Signal Space Projection (first four SSPs) was applied to reduce environmental noise.*

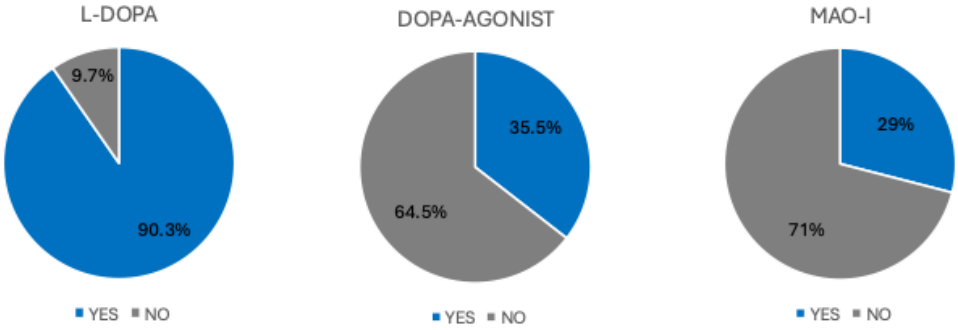

Figure S2*. Distribution of prescribed medication for Parkinson's disease symptoms. L-DOPA, levodopa; D-AGONIST, dopamine agonist; MAOI, monoamine oxidase inhibitor.*

Table S1. Detailed demographics.

ID	Group	UPDRS-III	H & Y	MDI	MoCA	PD dx	L-DOPA	DOPA-AGONIST	MAO-I
1	PD	20	1	4	29	3	YES	YES	NO
2	PD	22	1	6	30	1	YES	NO	YES
3	control	NA	NA	3	30	NA	NA	NA	NA
4	PD	25	1	8	30	3	NO	YES	NO
5	control	NA	NA	2	28	NA	NA	NA	NA
6	PD	27	1	6	30	1	YES	NO	YES
7	PD	39	2	0	30	15	YES	YES	YES
8	PD	28	1	8	29	9	YES	NO	NO
9	PD	39	2	5	29	10	YES	NO	YES
10	PD	38	2	5	27	5	YES	YES	YES
11	PD	40	2	5	27	12	YES	NO	NO
12	PD	23	1	3	29	10	YES	YES	NO
13	PD	31	2	4	28	12	YES	NO	NO
14	PD	38	2	10	28	3	NO	YES	NO
15	PD	38	2	15	27	6	YES	YES	YES
16	control	NA	NA	4	30	NA	NA	NA	NA
17	control	NA	NA	3	29	NA	NA	NA	NA
18	PD	24	1	11	30	2	YES	NO	NO
19	control	NA	NA	7	29	NA	NA	NA	NA
20	control	NA	NA	1	27	NA	NA	NA	NA
21	PD	39	2	10	29	17	YES	YES	YES
22	control	NA	NA	2	27	NA	NA	NA	NA
23	control	NA	NA	4	30	NA	NA	NA	NA
24	PD	35	2	4	29	2	YES	YES	YES
25	PD	26	2	3	28	1	YES	NO	NO
26	control	NA	NA	2	28	NA	NA	NA	NA
27	PD	13	1	11	27	3	NO	YES	YES
28	PD	26	2	15	27	3	YES	NO	NO
29	control	NA	NA	5	30	NA	NA	NA	NA
30	control	NA	NA	13	28	NA	NA	NA	NA
31	control	NA	NA	7	28	NA	NA	NA	NA
32	control	NA	NA	3	29	NA	NA	NA	NA
33	control	NA	NA	0	30	NA	NA	NA	NA
34	control	NA	NA	10	29	NA	NA	NA	NA
35	PD	23	2	7	26	5	YES	YES	NO
36	PD	37	2	12	28	1	YES	NO	NO
37	control	NA	NA	2	29	NA	NA	NA	NA
38	control	NA	NA	19	27	NA	NA	NA	NA
39	control	NA	NA	1	26	NA	NA	NA	NA
40	PD	41	2	17	28	4	YES	NO	NO
41	control	NA	NA	3	28	NA	NA	NA	NA
42	PD	30	2	8	30	7	YES	NO	NO

43	PD	47	2	10	27	14	YES	NO	NO
44	PD	31	2	13	30	5	YES	NO	NO
45	control	NA	NA	2	26	NA	NA	NA	NA
46	PD	34	2	8	30	8	YES	NO	NO
47	PD	29	2	8	27	2	YES	NO	NO
48	control	NA	NA	17	28	NA	NA	NA	NA
49	PD	43	2	9	29	2	YES	NO	NO
50	PD	26	2	15	30	4	YES	NO	NO
51	PD	25	2	4	27	4	YES	NO	NO
52	control	NA	NA	0	27	NA	NA	NA	NA
53	control	NA	NA	3	29	NA	NA	NA	NA
54	PD	43	2	5	28	2	YES	NO	NO
55	control	NA	NA	5	30	NA	NA	NA	NA
56	control	NA	NA	0	29	NA	NA	NA	NA
57	control	NA	NA	4	29	NA	NA	NA	NA

PD, Parkinson's disease; MDI, Major Depression Inventory; MoCA, Montreal Cognitive Assessment; PD dx, years since PD diagnosis; UPDRS-III, Motor Examination of the Movement Disorder Society Unified Parkinson's Disease Rating Scale; H & Y, Hoehn and Yahr scale; L-DOPA, levodopa; DOPA-AGONIST, dopamine agonist; MAOI, monoamine oxidase inhibitor.